

EfficientHRNet: Efficient Scaling for Lightweight High-Resolution Multi-Person Pose Estimation

Christopher Neff*, Aneri Sheth*, Steven Furgurson, and Hamed Tabkhi
{cneff1, asheth2, sfurgurs, htabkhiv}@uncc.edu

University of North Carolina at Charlotte

Abstract. Recent years have brought great advancement in 2D human pose estimation. However, bottom-up approaches that do not rely on external detectors to generate person crops, tend to have large model sizes and intense computational requirements, making them ill-suited for applications where large computation costs can be prohibitive. Lightweight approaches are exceedingly rare and often come at the price of massive accuracy loss. In this paper, we present EfficientHRNet, a family of lightweight 2D human pose estimators that unifies the high-resolution structure of state-of-the-art HigherHRNet [1] with the highly efficient model scaling principles of EfficientNet [2] to create high accuracy models with significantly reduced computation costs compared to other state-of-the-art approaches. In addition, we provide a formulation for jointly scaling our backbone EfficientNet below the baseline B0 and the rest of EfficientHRNet with it. Ultimately, we are able to create a family of highly accurate and efficient 2D human pose estimators that is flexible enough to provide a lightweight solution for a variety of application and device requirements. Baseline EfficientHRNet achieves a 0.4% accuracy improvement when compared to HRNet [1] while having a 34% reduction in floating point operations. When compared to Lightweight OpenPose [3], a compressed network designed specifically for lightweight inference, one EfficientHRNet model outperforms it by over 10% in accuracy while reducing overall computation by 15%, and another model, while only having 2% higher accuracy than Lightweight OpenPose, is able to further reduce computational complexity by 63%. At every level, EfficientHRNet proves to be more computationally efficient than other bottom-up 2D human pose estimation approaches, while achieving highly competitive accuracy.

1 Introduction

Two-dimensional human pose estimation is a common task used in many popular smart applications and has made substantial progress in recent years. There are two primary approaches to 2D human pose estimation. The first is a top-down approach, where cropped images of humans are provided and the network uses those cropped images to produce human keypoints. Top-down approaches rely

* These authors have equal contribution.

on object detectors to provide initial human crops, thus they often come with relatively higher computation cost, and are not truly end-to-end. The second is a bottom-up approach, where a network works off the original image and produces human keypoints for all people in the image. While these methods often do not quite reach the accuracy that is possible with state-of-the-art top-down approaches, they come with relatively lower model size and computational overhead.

Even so, state-of-the-art bottom-up approaches are still quite large and computationally expensive. The current state-of-the-art [1] having 63.8 million parameters and requiring 154.3 billion floating-point operations. Even though many emerging applications, such as self-driving vehicles, intelligent surveillance, and augmented reality, require lightweight multi-person human pose estimation, there has been much less attention towards developing lightweight bottom-up methods. This means that if an application’s real-time requirements and resource constraints do not match up well to the existing models, then a sub-optimal solution is the only available choice. To address this gap, there is a need for a family of lightweight human pose estimation models that achieves comparable accuracy to the state-of-the-art approaches.

In this paper, we present EfficientHRNet, a family of lightweight scalable networks for high-resolution and efficient bottom-up multi-person pose estimation. EfficientHRNet unifies the principles of state-of-the-art EfficientNet and HRNet, and presents a new formulation that enables near state-of-the-art human pose estimation while being more computationally efficient than all other bottom-up methods. Similar to HRNet, EfficientHRNet uses multiple resolutions of features to generate keypoints, but in a much more efficient manner. At the same time, it uses EfficientNet as a backbone and adapts its scaling methodology to be better suited for human pose estimation. To enable agile lightweight execution, EfficientHRNet further expands the EfficientNet formulation to not only scale below the baseline, but also to jointly scale down the input resolution, High-Resolution Network, and Heatmap Prediction Network. Through this, we are able to create a family of networks that can address the entire domain of lightweight 2D human pose estimation while being flexible towards the accuracy and computation requirements of an application. We evaluate our models on the COCO dataset [4]. Fig. 1 demonstrates how our models provide equivalent or higher accuracy at lower computational costs than their

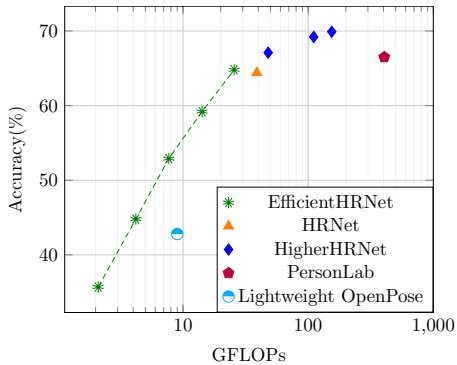


Fig. 1: A comparison of computational complexity and accuracy between bottom-up human pose estimation methods. Accuracy measured on COCO2017 val dataset. X-axis is logarithmic in scale.

direct peers. When comparing to state-of-the-art models, baseline EfficientNet competes in accuracy while requiring much less computation. Compared to HRNet [5], EfficientHRNet achieves 0.4% higher accuracy while requiring only 66% the number of operations. When comparing to HigherHRNet [1] and PersonLab [6], EfficientHRNet sees between a 1.7% to 5.1% decrease in accuracy, while only requiring between 7% to 17% of the computation. Even when comparing to models designed specifically for lightweight execution, such as Lightweight OpenPose [3], a scaled down EfficientHRNet is able to achieve 10.1% higher accuracy while further reducing computation by 15%. In addition, the scaled-down backbone models have been evaluated in isolation on ImageNet. The results demonstrate a competitive accuracy while achieving greater efficiency than their peers.

In summary, our contributions are as follows:

- We propose a family of efficient and scalable models called EfficientHRNet for 2D human pose estimation unifying the principles of recently introduced EfficientNet and HRNet.
- We provide a new formulation for scaling EfficientNet below the baseline B0 model to achieve highly accurate and lightweight pose estimation suitable for applications that require low computation costs.
- Our quantitative and qualitative results on COCO dataset demonstrate near state-of-the-art accuracy while being more computationally efficient than comparable methods.

2 Related Work

This section first presents related work relevant to the field of top-down and bottom-up methods for 2D human pose estimation. Then, a survey on multi-scale high-resolution networks, particularly for computer vision applications, is presented. Lastly, popular model scaling techniques that have emerged in recent years are discussed.

2.1 Top-down Methods

Top-down methods rely on first identifying all the persons in an image using an object detector, and then detecting the keypoints for a single person within a defined bounding box. These single person [7], [8], [9], [10], [11], [12], [13], [14], [15], [16], [17] and multi-person [18], [19], [20], [21], [22] pose estimation methods often generate person bounding boxes using object detector [23], [24], [25], [26]. For instance, RMPE [21] adds symmetric spatial transformer network on top of single person pose estimator stacked hourglass network [14] to get high-quality regions from inaccurate bounding boxes and then detects poses using parametric non-maximum suppression.

2.2 Bottom-up Methods

Bottom-up methods [27], [28], [29], [30], [6], [31], [32], [33], [34], [35] first detect identity-free keypoints in an image and then group them into persons using various keypoints grouping techniques. Methods like [32] and [33] perform

grouping by integer linear program and non-maximum suppression. This allows for much faster inference times as compared to top-down methods with almost similar accuracies. Other methods further improve upon prediction time by using greedy grouping techniques, along with other optimizations, as seen in [27], [28], [29], [30], [6]. For instance, OpenPose [27], [28] is a multi-stage network where one branch detects keypoints in the form of heatmaps, while the other branch generates Part Affinity Fields that are used to associate keypoints with each other. Grouping is done by calculating the line integral between all keypoints and grouping the pair that has the highest integral. Lightweight OpenPose [3] replaces larger backbone with MobileNets to achieve real-time performance with fewer parameters and FLOPs while compromising on accuracy. PifPaf [29] uses Part *Intensity* Fields to detect body parts and Part *Associative* Fields for associating parts with each other to form human poses. In [30], a stacked hour-glass network [14] is used both for predicting heatmaps and grouping keypoints. Grouping is done by assigning each keypoint with an embedding, called a tag, and then associating those keypoints based on the L_2 distance between the tag vectors. In this paper, we mainly focus on a highly accurate, end-to-end multi-person pose estimation method as in [30].

2.3 Multi-scale High-Resolution Networks

Feature pyramid networks augmented with multi-scale representations are widely adopted for complex and necessary computer vision applications like segmentation and pose estimation [36], [37], [38], [39], [40], [41]. Recovering high-resolution feature maps using techniques like upsampling, dilated convolution, and deconvolution are also widely popular for object detection [39], semantic segmentation [42], [43], [44], [45], [46], [47], [48], [49], [50], [51], [52] and pose estimation [14], [53,54], [55], [56], [40], [41], [57], [32], [33]. Moreover, there are several works that focus on generating high-resolution feature maps directly [58], [59], [60], [61], [62], [63], [5], [1]. HRNet [5], [63] proposes to maintain high-resolution feature maps throughout the entire network. HRNet consists of multiple branches with different resolutions across multiple stages. With multi-scale fusion, HRNet is able to generate high resolution feature maps and has found its application in object detection, semantic segmentation, and pose estimation [5], [62], [63] thereby achieving remarkable accuracies. Recently, HigherHRNet for multi-person pose estimation [1] is proposed which uses HRNet as base network to generate high resolution feature maps, and further adds a deconvolution module to predict accurate, high-quality heatmaps. HigherHRNet achieves state-of-the-art accuracy on the COCO dataset [4], surpassing all existing bottom-up methods. In our paper, we adopt the principles of HigherHRNet for generating high-resolution feature maps with multi-scale fusion for predicting high-quality heatmaps.

2.4 Model Scaling

Previous works on bottom-up pose estimation [27], [28], [1], [5], [30], [14] often rely on either large backbone networks, like ResNet [64] or VGGNet [65], or large input resolutions and multi-scale training for achieving state-of-the-art accuracy.

Some recent works [5],[1] show that increasing the channel dimension of otherwise identical models can further improve accuracy. EfficientNet [2] and RegNet [66] show that by jointly scaling network width, depth, and input resolution, better efficiency for image classification can be achieved compared to previous state-of-the-art networks using much larger models. More recently, EfficientNet’s lite models remove elements, such as squeeze and excite and swish layers, to make the network more hardware friendly. Inspired by EfficientNet, EfficientDet [67] proposes a compound scaling method for object detection along with efficient multi-scale feature fusion. We observe that there is a lack of an efficient scaling method for multi-person pose estimation, especially for embedded devices. Lightweight pose estimation models which are scalable and comparatively accurate are needed for computer vision applications which focus on real-time performance. Our proposed compound scaling, also inspired by EfficientNet, is a method that jointly scales the width, depth, and input resolution of our network, as well as the repetition within our *high-resolution modules*, explained in Section 3. In addition, this compound scaling allows our EfficientNet backbone to scale below the baseline B0, creating even lighter weight models.

3 EfficientHRNet

We have developed a family of scalable and lightweight multi-person pose estimation models called EfficientHRNet. Fig. 2 describes the overall architecture of our approach. In this section, we will firstly give a brief review of our proposed architecture and then we will introduce our new compound scaling method for EfficientHRNet.

3.1 Network Architecture and Formulation

EfficientHRNet comprises of three sub-networks: (1) Backbone Network, (2) High-Resolution Network, and (3) Heatmap Prediction Network for human pose estimation. The first stage of the network is the backbone, consisting of EfficientNet [2]. The backbone EfficientNet model outputs four different resolution feature maps of decreasing resolutions $\frac{1}{4}$, $\frac{1}{8}$, $\frac{1}{16}$, and $\frac{1}{32}$ the size of the input image. These feature maps are passed into the main body of the network, called the High-Resolution Network. The High-Resolution Network is inspired by HRNet [5], [63] and HigherHRNet [1]. Borrowing the principles of these higher resolution networks brings two major advantages:

- (i) By maintaining multiple high-resolution feature representations throughout the network, heatmaps with a higher degree of spatial precision are generated.
- (ii) Repeated multi-scale fusions allow for high-resolution feature representations to inform lower-resolution feature representations, and vice versa, resulting in robust, multi-resolution feature representations that are ideal for multi-person human pose estimation.

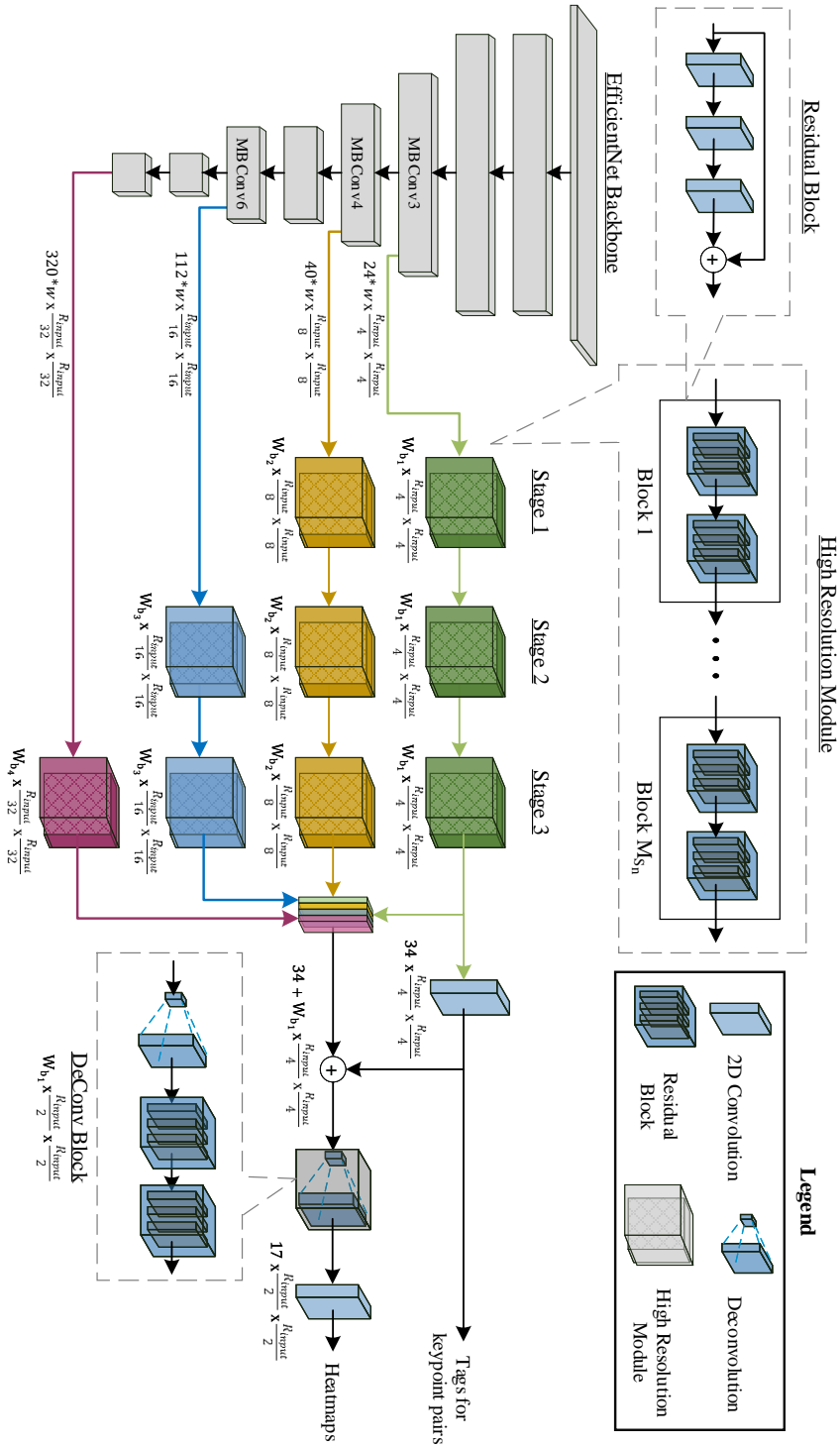


Fig. 2: A detailed illustration of the EfficientHRNet architecture. Consisting of a backbone EfficientNet, a High-Resolution Network with three stages and four branches (denoted by different colors), and a Heatmap Prediction Network. EfficientHRNet is completely scalable, allowing network complexity to be customized for target applications.

Fig. 2 presents a detailed architecture illustration of EfficientHRNet. It shows the three sub-networks - the Backbone Network, the High-Resolution Network, and the Heatmap Prediction Network - in detail. It also provides equations showing how the network scales the input resolution R_{input} and width of feature maps W_{b_n} , which will be further explained in Section 3.2.

As seen in Fig. 2, the High-Resolution Network has three stages s_1 , s_2 , and s_3 , containing four parallel branches b_1 , b_2 , b_3 , and b_4 of different resolutions. The first stage s_1 starts with two branches b_1 and b_2 , with each consecutive stage adding an additional branch, until all four branches are present in s_3 . These four branches each consist of *high resolution modules* with a width of W_{b_n} . Each branch b_n contains feature representations of decreasing resolutions that mirror the resolutions output by the Backbone Network, as shown in Fig. 2 and the following equation:

$$W_{b_n} \times \frac{R_{input}}{2^n + 1} \quad (1)$$

For instance, stage 2 (s_2) has three branches of resolutions $\frac{1}{4}$, $\frac{1}{8}$, and $\frac{1}{16}$ of the original input image resolution and a width W_{b_n} as seen in Fig. 2. Moreover, each *high resolution module* is made up of a number of blocks, M_{s_n} , each containing two *residual blocks*, each performing three convolution operations with a residual connection.

In order to predict more accurate heatmaps, a *DeConv block* is added on top of the High-Resolution Network, as proposed in [1]. Transposed convolution is used to generate high quality feature maps which are $\frac{1}{2}$ the original input resolution. The input to the *DeConv block* is the concatenation of the feature maps and predicted heatmaps from the High-Resolution Network, as shown in the equation below:

$$34 + W_{b_1} \times \frac{R_{input}}{4} \times \frac{R_{input}}{4} \quad (2)$$

Two *residual blocks* are added after the *DeConv block* to refine the up-sampled feature maps, as seen in Fig. 2.

Lastly, the Heatmap Prediction Network is used to generate human keypoint predictions. After the end of the *DeConv block*, a 1x1 convolution is used to predict heatmaps and tagmaps in a similar fashion to [30], the feature map size of each shown below:

$$\begin{aligned} T_{size} &= 34 \times \frac{R_{input}}{4} \times \frac{R_{input}}{4} \\ H_{size} &= 17 \times \frac{R_{input}}{2} \times \frac{R_{input}}{2} \end{aligned} \quad (3)$$

The grouping process clusters keypoints into multiple persons by grouping keypoints whose tags have minimum L_2 distance. Moreover, much like [1], our network is scale-aware and uses multi-resolution supervision for heatmaps during training to allow the network to learn with more precision, even for small-scale persons. From the ground truth, heatmaps for different resolutions are generated to match the predicted keypoints of different scales. Thus, the final heatmaps

loss is the sum of mean squared errors for all resolutions. However, as high resolutions tagmaps do not converge well, tagmaps are trained on a resolution $\frac{1}{4}$ of the original input resolution, as in [30].

3.2 Compound Scaling Method

In this part, the compound scaling method is described, which jointly scales all parts of EfficientHRNet, as seen in Fig. 2. Our aim is to develop a family of models optimized for both accuracy and efficiency, which can be scaled to meet a diverse set of memory and compute constraints.

Previous works on bottom-up pose estimation mostly scale the base network by using bigger backbone networks like ResNet [64] and VGGNet [65], using large input image sizes, or using multi-scale training to achieve high accuracies. However, these methods rely on scaling only a single dimension, which has limited effectiveness. Recent works [2], [66] show notable performance on image classification by jointly scaling the width, depth, and input image resolution. Inspired by EfficientNet, EfficientDet [67] proposes a similar compound scaling method for object detection, which jointly scales the backbone network, multi-scale feature network, and the object detector network. We propose a heuristic-based compound scaling method for bottom-up pose estimation, based on [2], [67], using a scaling coefficient ϕ to jointly scale the Backbone Network, the High-Resolution Network, and the Heatmap Prediction Network. More precisely, we scale the EfficientNet backbone below the baseline and scale down the overall network in order to maintain near state-of-the-art accuracy while creating lightweight and flexible networks.

Backbone Network. We maintain the same width and depth scaling coefficients as EfficientNet [2]. In order to meet the demands of running models on constrained devices, a new formulation for scaling EfficientNet below the baseline into a more compact model is provided.

Starting with the baseline EfficientNet-B0 scaling coefficients:

$$\begin{aligned} \text{depth} : d &= 1.2^\phi \\ \text{width} : w &= 1.1^\phi \\ \text{resolution} : r &= 1.15^\phi \end{aligned} \tag{4}$$

we invert ϕ , i.e. $\phi = -1, -2, -3, -4$, to calculate the scaling multipliers for the compact EfficientNet models, which we call B_{-1}, B_{-2}, B_{-3} and B_{-4} respectively. As an example, in order to take the baseline resolution, 224, and scale it down for our B_{-1} model, we would take r , from eq. 4, with $\phi = -1$. This would result in a resolution scaling coefficient of 1.15^{-1} , i.e. 0.87, leaving a scaled resolution size of $\text{ceil}(224 * 0.87) = 195$. This pattern repeats for $B_{-2} - B_{-4}$, and can be seen in Table 2. We train these compact EfficientNet models (B_{-1} to B_{-4}) on ImageNet and use the resulting weights for the Backbone Network in EfficientHRNet models.

High-Resolution Network. The High-Resolution Network has three stages and four branches with four different feature map sizes. Each branch n also has

Model	Input size (R_{input})	Backbone network	Width per branch ($W_{b_1}, W_{b_2}, W_{b_3}, W_{b_4}$)	# blocks per stage ($M_{s_2}, M_{s_3}, M_{s_4}$)	Tags (T_{size})	Heatmaps (H_{size})
H_0 ($\phi = 0$)	512	B_0	32, 64, 128, 256	1, 4, 3	128	256
H_{-1} ($\phi = -1$)	480	B_{-1}	26, 52, 103, 206	1, 3, 3	120	240
H_{-2} ($\phi = -2$)	448	B_{-2}	21, 42, 83, 166	1, 2, 3	112	224
H_{-3} ($\phi = -3$)	416	B_{-3}	17, 34, 67, 133	1, 1, 3	104	208
H_{-4} ($\phi = -4$)	384	B_{-4}	14, 27, 54, 107	1, 1, 2	96	192

Table 1: Efficient scaling configs for EfficientHRNet

a different width W_{b_n} and our baseline H_0 model has a width of 32, 64, 128, and 256 for each branch respectively. We selectively pick a width scaling factor of 1.25 and scale down the width using the following equation:

$$W_{b_n} = (n \cdot 32) \cdot (1.25)^\phi \quad (5)$$

where n is a particular branch number and ϕ is our compound scaling coefficient. Furthermore, within each stage, each *high resolution module* has multiple *blocks* M_{s_n} which repeat a number of times, as seen in Table 1. In our baseline H_0 model, *blocks* within each stage repeat 1, 4, and 3 times respectively. We found that the number of repetitions in stage 3 had the largest impact on accuracy. Therefore, the number of repetitions within a *high resolution module* M_{s_2} decreases linearly as we scale down our models, starting with stage 2 until reaching a single repetition and then moving on to stage 3, as shown in Table 1.

Heatmap Prediction Network. The *DeConv block* is scaled in the same manner as the width of the High Resolution Network (5). The Heatmap Prediction Network outputs tags and heatmaps whose width remains fixed across all our models.

Input Image Resolution. The EfficientNet layers downsample the original input image resolution by 32 times. Thus, the input resolution of EfficientHRNet must be dividable by 32, and is linearly scaled down as shown in equation (6).

$$R_{input} = 512 + 32 \cdot \phi \quad (6)$$

Based on equations (4), (5), and (6), we have developed a group of pose estimation models from H_0 to H_{-4} called EfficientHRNet, as shown in Table 1.

4 Experimental Results

In this section, we first evaluate our method of scaling EfficientNet below the baseline through classification on the popular ImageNet [68] and CIFAR-100 [69] datasets. Then, we conduct an exhaustive evaluation of five different EfficientHRNet models on the challenging COCO dataset and compare to state-of-the-art methods. Finally, we present a qualitative evaluation of EfficientHRNet, illustrating both where the models excel and where they fall short.

4.1 Classification for Compact EfficientNet

Dataset. ImageNet [68] has been a long time standard benchmark for object classification and detection thanks to its annual contest, the ImageNet Large

Scale Visual Recognition Challenge, that debuted in 2010. The challenge uses a subset of the full dataset with over a million images spread out over 1000 object classes. For training, validating, and testing purposes, the trimmed ImageNet is divided into three sets: 800k images will be used for training the network, 150k will be used for validation after each epoch, and 50k will be used for testing the fully trained model. CIFAR-100 [69] consists of 100 object classes each with 500 images for training, and 100 for testing. This relatively small dataset helps illuminate our lightweight models, which start to struggle with the larger ImageNet as ϕ decreases, designed for resource constrained devices that might not need to classify as many object classes.

Training. We use random rotation, random scale, and random aspect ratio to crop the input images to the desired resolutions based on the current EfficientNet model. Color jitter was also used to randomly change the brightness, contrast, saturation, and hue of the RGB channels using principle component analysis [70]. The images are then normalized using per channel mean and standard deviation. Each model was trained using Stochastic Gradient Descent [71] with a weight decay of $1e - 4$. The weights were initialized using the Xavier algorithm [72] and underwent five warm-up epochs with a learning rate of $1e - 4$ that increased linearly until it reached 0.05. The networks were then trained for an additional 195 epochs and followed the step decay learning rate scheduler [73] that reduces the learning rate by a factor of 10 every 30 epochs.

Testing. The compact EfficientNet models were tested for accuracy based on their respective testsets. For a fair comparison, the number of ImageNet test samples were reduced to 10,000 to match the test set of CIFAR-100, where the batch size is set to 1. These results can be seen in Table 2.

Results on ImageNet and CIFAR-100. Looking at B_{-1} we see a 15% reduction in parameters and 25% reduction in operations, yet an accuracy drop of only 1.2% and 0.5% on ImageNet and CIFAR-100 respectively. More impressively, B_{-2} sees a 35-40% reduction in parameters and a 50% reduction in operations, yet only a 3.7% and 2.1% drop in accuracy on the two datasets. This minor accuracy loss is negligible compared to the massive reduction in model size and computation, allowing for much faster inference as well as deployment on low-power and resource constrained devices. In the most extreme, B_{-4} shows a parameter reduction of 68-75% and a 87.5% decrease in operations while having an accuracy drop of 9.4% and 7.6% on ImageNet and CIFAR-100. While the accuracy drop is a bit more significant here, the massive reduction in computation allows for much more flexibility when it comes to deployment in systems where

Model	Input size	ImageNet			CIFAR-100		
		# Params	FLOPS	Top-1	# Params	FLOPS	Top-1
B_0 ($\phi = 0$)	224	5.3M	0.4B	75	4.1M	0.4B	81.9
B_{-1} ($\phi = -1$)	195	4.5M	0.3B	73.8	3.5M	0.3B	81.4
B_{-2} ($\phi = -2$)	170	3.4M	0.2B	71.3	2.5M	0.2B	79.8
B_{-3} ($\phi = -3$)	145	2.8M	0.1B	68.5	1.9M	0.1B	78.2
B_{-4} ($\phi = -4$)	128	1.3M	0.05B	65.6	1.3M	0.05B	74.3

Table 2: Compact EfficientNet performance on ImageNet and CIFAR-100 datasets.

a lightweight approach is needed. This gives us a solid foundation on which to build EfficientHRNet.

4.2 2D Human Pose Estimation for EfficientHRNet

Dataset. COCO dataset [4] has over 200,000 images with 250,000 person instances each labeled with 17 keypoints. The COCO dataset has three sets - *train* set with 57k images, *val* set with 5k images and *test*, which is divided into *test-dev* with 20k images and *test-challenge* with 20k images. We perform all our training on *train* set, report our results on *val* set, and compare with state-of-the-art methods on *test-dev* set for a fair comparison.

Evaluation. The COCO evaluation defines object keypoint similarity (OKS), and uses mean average precision (AP) over 10 OKS thresholds as the main evaluation metric¹. The OKS is calculated from the scale of the person and the Euclidean distance between the GT and predicted points, similar to IoU in object detection. For our results, we report average precision and recall scores: AP (mean of AP scores at OKS = 0.50, 0.55, \dots , 0.90, 0.95), AP⁵⁰ (AP at OKS = 0.50), AP⁷⁵, AP^M for medium objects, AP^L for large objects, and AR (mean of recall scores).

Training. We use random rotation, random scale, and random translation for data augmentation to crop the input images to a fixed input resolution depending on the EfficientHRNet model. Following HigherHRNet [1], we generate two ground truth heatmaps of different sizes, $\frac{1}{2}$ and $\frac{1}{4}$ of the original input size respectively. Each EfficientHRNet model is trained using Adam optimizer [74] and weight decay of $1e-4$. All models from H_0 to H_{-4} are trained for a total of 300 epochs with a base learning rate of $1e-3$, decreasing to $1e-4$ and $1e-5$ at 200th and 260th epochs respectively. To maintain balance between heatmaps loss and grouping loss, we weight the losses at 1 and $1e-3$ respectively

Testing. For testing on COCO *val* and *test-dev* sets, we resize the short side of test input image to match our input resolution while preserving the aspect ratio. As in HigherHRNet [1], heatmap aggression is done by resizing the predicted

¹ <http://cocodataset.org/#keypoints-eval>

Model	Input size	single-scale			multi-scale			# Params	FLOPs
		AP	AP ⁵⁰	AP ⁷⁵	AP	AP ⁵⁰	AP ⁷⁵		
PersonLab	1401	66.5	86.2	71.9	-	-	-	68.7M	405.5B
HRNet	512	64.4	-	-	-	-	-	28.5M	38.9B
HigherHRNet	512	67.1	86.2	73.0	69.9	87.1	76.0	28.6M	47.9B
Lightweight OpenPose	368	42.8	-	-	-	-	-	4.1M	9.0B
H_0 ($\phi = 0$)	512	64.8	85.3	70.7	68.1	87.0	74.1	23.3M	25.6B
H_{-1} ($\phi = -1$)	480	59.2	82.6	64.0	63.2	84.3	68.6	16M	14.2B
H_{-2} ($\phi = -2$)	448	52.9	80.5	59.1	56.4	82.2	63.4	10.3M	7.7B
H_{-3} ($\phi = -3$)	416	44.8	76.7	48.2	46.4	76.6	50.8	6.9M	4.2B
H_{-4} ($\phi = -4$)	384	35.7	69.6	33.7	40.3	73.0	41.9	3.7M	2.1B

Table 3: Comparisons with bottom-up methods on COCO2017 val dataset

heatmaps to the input resolution and taking the average. We test our models using both single scale and multi-scale heatmaps, as is common. Following [30], we average the output detection heatmaps across different scales and concatenate the tags into higher dimensional tags, making different objects and persons considerably more scale-invariant.

Results on COCO2017 *val*. We report EfficientHRNet H_0 to H_{-4} accuracy on COCO *val* set along with parameters and FLOPs of the entire network and compare it with other bottom-up methods. As summarized in Table 3, our baseline H_0 model outperforms HRNet [1] with 0.4% more accuracy, 18% fewer parameters and 34% fewer FLOPs. Our H_{-2} and H_{-3} models outperform Lightweight OpenPose [3] in accuracy while having fewer FLOPs. H_{-4} has the worst accuracy of any model in Table 3, however it boasts both the smallest model size and fewest number of operations, that later seeing an over 75% reduction from its lightest weight competitor. This makes our scaled-down models the new state-of-the-art for lightweight bottom-up human pose estimation.

Results on COCO2017 *test-dev*. Table 4 compares EfficientHRNet with other bottom-up pose estimation methods on COCO *test-dev* set. Our baseline H_0 model with single-scale testing serves as an efficient and accurate model for bottom-up methods as it is almost comparable to HRNet [1] in accuracy, losing by only 0.1%, while having a smaller model size and fewer FLOPs. H_0 outperforms Hourglass [14] in both single-scale and multi-scale testing by 7.4%

Method	Backbone	Input size	# Params	FLOPs	AP	AP ⁵⁰	AP ⁷⁵	AP ^M	AP ^L	AR
w/o multi-scale test										
OpenPose	-	-	25.94M	160B	61.8	84.9	67.5	57.1	68.2	66.5
Hourglass	Hourglass	512	277.8M	206.9B	56.6	81.8	61.8	49.8	67.0	-
PersonLab	ResNet-152	1401	68.7M	405.5B	66.5	88.0	72.6	62.4	72.3	-
PifPaf	ResNet-152	-	-	-	66.7	-	-	62.4	72.9	-
HRNet	HRNet-W32	512	28.5M	38.9B	64.1	86.3	70.4	57.4	73.9	-
HigherHRNet	HRNet-W32	512	28.6M	47.9B	66.4	87.5	72.8	61.2	74.2	-
HigherHRNet	HRNet-W48	640	63.8M	154.3B	68.4	88.2	75.1	64.4	74.2	-
H_0 ($\phi=0$)	B_0	512	23.3M	25.6B	64.0	86.2	70.1	59.1	71.1	69.1
H_{-1} ($\phi=-1$)	B_{-1}	480	16M	14.2B	59.1	83.9	66.4	54.6	65.7	64.7
H_{-2} ($\phi=-2$)	B_{-2}	448	10.3M	7.7B	52.8	82.3	58.5	47.3	60.6	59.1
H_{-3} ($\phi=-3$)	B_{-3}	416	6.9M	4.2B	44.5	78.0	47.6	39.8	51.0	51.8
H_{-4} ($\phi=-4$)	B_{-4}	384	3.7M	2.1B	35.5	71.1	32.5	29.9	43.5	42.8
w/ multi-scale test										
Hourglass	Hourglass	512	277.8M	206.9B	63.0	85.7	68.9	58.0	70.4	-
Hourglass	Hourglass	512	277.8M	206.9B	65.5	86.8	72.3	60.6	72.6	70.2
PersonLab	ResNet-152	1401	68.7M	405.5B	68.7	89.0	75.4	64.1	75.5	75.4
HigherHRNet	HRNet-W48	640	63.8M	154.3B	70.5	89.3	77.2	66.6	75.8	74.9
H_0 ($\phi=0$)	B_0	512	23.3M	25.6B	67.1	88.1	73.6	63.2	72.5	71.8
H_{-1} ($\phi=-1$)	B_{-1}	480	16M	14.2B	62.3	85.1	67.8	58.2	67.8	67.4
H_{-2} ($\phi=-2$)	B_{-2}	448	10.3M	7.7B	55.0	83.1	61.8	51.4	60.0	61.4
H_{-3} ($\phi=-3$)	B_{-3}	416	6.9M	4.2B	45.5	78.2	49.4	42.7	48.9	53.1
H_{-4} ($\phi=-4$)	B_{-4}	384	3.7M	2.1B	39.7	74.2	39.7	35.7	45.5	47.0

Table 4: Comparisons with state-of-the-art bottom-up methods on COCO2017 test-dev dataset.

and 1.6% respectively, with H_0 remarkably having about 10% the model size and number of FLOPs as Hourglass. In all cases where H_0 loses in accuracy, it more than makes up for it in a reduction in parameters and operations. Additionally, our H_{-1} model, with only 16M parameters and 14.2B FLOPs, outperforms both OpenPose [27, 28] and Hourglass [14], demonstrating EfficientHRNet’s efficiency and suitability for low-power and resource constrained devices. As we scale down EfficientHRNet using our compound scaling method, we see somewhat minor drops in accuracy with significant drops parameters and FLOPs as compared to our baseline H_0 model. H_{-1} has 31.3% less parameters and 44.5% less FLOPs as compared to H_0 while only being 4.9% less accurate. Similarly, our lightest model H_{-4} is 84% smaller and has 91.7% less FLOPs, with a less than 45% drop in accuracy. Interestingly, EfficientHRNet is the only bottom-up pose estimator that is able to provide such lightweight models while still having accuracies that are comparable to state-of-the-art bottom-up methods, as illustrated by both Table 4 and Fig. 1. These results nicely show the validity of our approach to scalability and efficiency in EfficientHRNet, and its suitability as a lightweight human pose estimator.

Qualitative Comparison. To show how EfficientHRNet models perform on COCO dataset, we present qualitative results on the *test-challenge* set. Fig. 3 shows simple, medium, and complex examples for all EfficientHRNet models from H_0 to H_{-4} . For the simple case, we see that a single person pose is correctly formed for all our models, but as we go towards smaller models, the detected keypoints distort the pose due to the drop in accuracy. In the case of medium complexity examples, where there is an occlusion over multiple persons, we observe that all our models are able to accurately detect different people in the image. However, smaller models, such as H_{-3} and H_{-4} , detect multiple key-

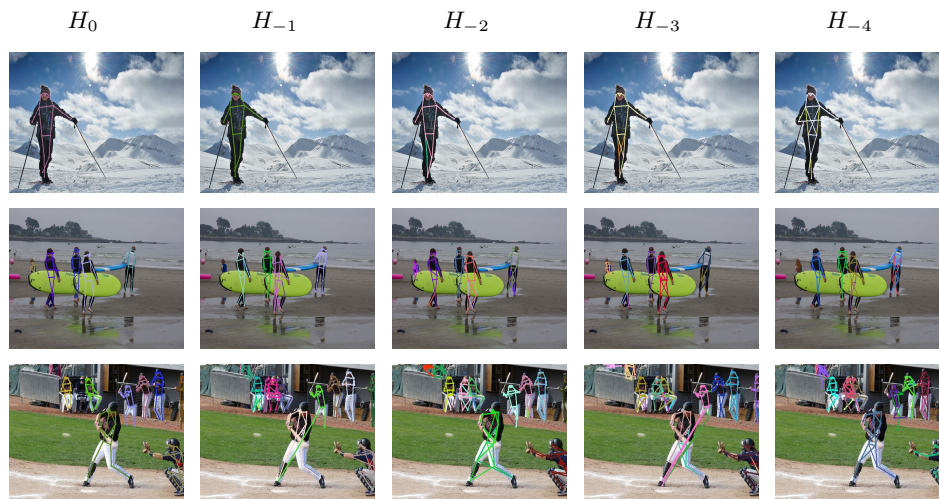


Fig. 3: Qualitative Results for EfficientHRNet models on COCO2017 test dataset. Top to bottom: Simple, Medium and Complex examples.

points for the same person, making the pose look clustered and creating noise. As far as complex examples are concerned, we show an image with more than 4 people, all in different poses at different distances from the camera. We observe that the quality of poses is affected but all the models are still able to identify all the humans in the image. The smaller models particularly struggle with merging keypoints across multiple people and detecting multiple keypoints for the same person, just as in the medium example. Our qualitative results nicely visualize the relationship between detected keypoints and model size, and show that the overall effect on accurate pose prediction is not significant in simple and medium examples as we go towards smaller models. However, complex scenes can still be a struggle for lightweight pose estimation, and additional post processing might be needed to redress the output for use in a real-world system.

5 Conclusion

In this paper, we have presented EfficientHRNet, a family of scalable networks for high-resolution and efficient bottom-up multi-person pose estimation, especially for low-power edge devices. We unify the principles of state-of-the-art EfficientNet and HRNet to create a network architecture for lightweight human pose estimation, and we propose a new compound scaling method that jointly scales down the input resolution, backbone network, and high-resolution feature network. EfficientHRNet is not only more efficient than all other bottom-up human pose estimation methods, but it can maintain accuracy competitive with state-of-the-art models on the challenging COCO dataset. Remarkably, EfficientHRNet can achieve this near state-of-the-art accuracy with fewer parameters and less computational complexity than other bottom-up multi-person pose estimation networks.

There are several directions in which this work could be continued in the future. In this article, we focused on lightweight human pose estimation, and thus only scaled our network down from the baseline. However, there is nothing preventing EfficientHRNet from being scaled to a larger network in a fashion more similar to EfficientNet [2] or EfficientDet [67]. In addition, the following principles are shown in EfficientNet-lite, certain architectural elements of the EfficientNet backbone, mainly the squeeze and excite layers, as well as the swish activation, could be removed or replaced. An exploration of how this impacts inference on different hardware would be a potential avenue of research. Finally, while we chose to focus on 2D human pose estimation, the principles and architecture of EfficientHRNet could be applied to numerous other computer vision tasks, such as object detection, semantic segmentation, and depth estimation, to name a few examples.

Acknowledgement

This research is supported by the National Science Foundation (NSF) under Awards No. 1737586 and 1831795.

References

1. Cheng, B., Xiao, B., Wang, J., Shi, H., Huang, T.S., Zhang, L.: Higherhrnet: Scale-aware representation learning for bottom-up human pose estimation (2019)
2. Tan, M., Le, Q.V.: Efficientnet: Rethinking model scaling for convolutional neural networks. CoRR **abs/1905.11946** (2019)
3. Osokin, D.: Real-time 2d multi-person pose estimation on CPU: lightweight open-pose. CoRR **abs/1811.12004** (2018)
4. Lin, T.Y., Maire, M., Belongie, S., Bourdev, L., Girshick, R., Hays, J., Perona, P., Ramanan, D., Zitnick, C.L., Dollr, P.: Microsoft coco: Common objects in context (2014)
5. Sun, K., Xiao, B., Liu, D., Wang, J.: Deep high-resolution representation learning for human pose estimation. CoRR **abs/1902.09212** (2019)
6. Papandreou, G., Zhu, T., Chen, L., Gidaris, S., Tompson, J., Murphy, K.: Personlab: Person pose estimation and instance segmentation with a bottom-up, part-based, geometric embedding model. CoRR **abs/1803.08225** (2018)
7. Yang, Y., Ramanan, D.: Articulated pose estimation with flexible mixtures-of-parts. In: CVPR 2011. (2011) 1385–1392
8. Dantone, M., Gall, J., Leistner, C., Van Gool, L.: Human pose estimation using body parts dependent joint regressors. In: 2013 IEEE Conference on Computer Vision and Pattern Recognition. (2013) 3041–3048
9. Johnson, S., Everingham, M.: Learning effective human pose estimation from inaccurate annotation. In: CVPR 2011. (2011) 1465–1472
10. Sapp, B., Taskar, B.: Modec: Multimodal decomposable models for human pose estimation. In: Proceedings / CVPR, IEEE Computer Society Conference on Computer Vision and Pattern Recognition. IEEE Computer Society Conference on Computer Vision and Pattern Recognition. (2013) 3674–3681
11. Gkioxari, G., Arbelaez, P., Bourdev, L., Malik, J.: Articulated pose estimation using discriminative armlet classifiers. In: Proceedings of the 2013 IEEE Conference on Computer Vision and Pattern Recognition. CVPR 13, USA, IEEE Computer Society (2013) 33423349
12. Toshev, A., Szegedy, C.: Deeppose: Human pose estimation via deep neural networks. CoRR **abs/1312.4659** (2013)
13. Jain, A., Tompson, J., Andriluka, M., Taylor, G., Bregler, C.: Learning human pose estimation features with convolutional networks. (2013)
14. Newell, A., Yang, K., Deng, J.: Stacked hourglass networks for human pose estimation. CoRR **abs/1603.06937** (2016)
15. Bulat, A., Tzimiropoulos, G.: Human pose estimation via convolutional part heatmap regression. CoRR **abs/1609.01743** (2016)
16. Belagiannis, V., Zisserman, A.: Recurrent human pose estimation. CoRR **abs/1605.02914** (2016)
17. Wei, S., Ramakrishna, V., Kanade, T., Sheikh, Y.: Convolutional pose machines. CoRR **abs/1602.00134** (2016)
18. Iqbal, U., Gall, J.: Multi-person pose estimation with local joint-to-person associations. CoRR **abs/1608.08526** (2016)
19. Papandreou, G., Zhu, T., Kanazawa, N., Toshev, A., Tompson, J., Bregler, C., Murphy, K.P.: Towards accurate multi-person pose estimation in the wild. CoRR **abs/1701.01779** (2017)
20. Huang, S., Gong, M., Tao, D.: A coarse-fine network for keypoint localization. (2017) 3047–3056

21. Fang, H., Xie, S., Tai, Y., Lu, C.: Rmpe: Regional multi-person pose estimation. In: 2017 IEEE International Conference on Computer Vision (ICCV). (2017) 2353–2362
22. Chen, Y., Wang, Z., Peng, Y., Zhang, Z., Yu, G., Sun, J.: Cascaded pyramid network for multi-person pose estimation. CoRR [abs/1711.07319](#) (2017)
23. Cheng, B., Wei, Y., Shi, H., Feris, R.S., Xiong, J., Huang, T.S.: Decoupled classification refinement: Hard false positive suppression for object detection. CoRR [abs/1810.04002](#) (2018)
24. Cheng, B., Wei, Y., Shi, H., Feris, R.S., Xiong, J., Huang, T.S.: Revisiting RCNN: on awakening the classification power of faster RCNN. CoRR [abs/1803.06799](#) (2018)
25. Lin, T., Dollár, P., Girshick, R.B., He, K., Hariharan, B., Belongie, S.J.: Feature pyramid networks for object detection. CoRR [abs/1612.03144](#) (2016)
26. Ren, S., He, K., Girshick, R.B., Sun, J.: Faster R-CNN: towards real-time object detection with region proposal networks. CoRR [abs/1506.01497](#) (2015)
27. Cao, Z., Simon, T., Wei, S., Sheikh, Y.: Realtime multi-person 2d pose estimation using part affinity fields. CoRR [abs/1611.08050](#) (2016)
28. Cao, Z., Hidalgo, G., Simon, T., Wei, S., Sheikh, Y.: Openpose: Realtime multi-person 2d pose estimation using part affinity fields. CoRR [abs/1812.08008](#) (2018)
29. Kreiss, S., Bertoni, L., Alahi, A.: Pifpaf: Composite fields for human pose estimation. CoRR [abs/1903.06593](#) (2019)
30. Newell, A., Deng, J.: Associative embedding: End-to-end learning for joint detection and grouping. CoRR [abs/1611.05424](#) (2016)
31. Andriluka, M., Roth, S., Schiele, B.: Pictorial structures revisited: People detection and articulated pose estimation. (2009) 1014 – 1021
32. Pishchulin, L., Insaftudinov, E., Tang, S., Andres, B., Andriluka, M., Gehler, P.V., Schiele, B.: Deepcut: Joint subset partition and labeling for multi person pose estimation. CoRR [abs/1511.06645](#) (2015)
33. Insaftudinov, E., Pishchulin, L., Andres, B., Andriluka, M., Schiele, B.: Deepercut: A deeper, stronger, and faster multi-person pose estimation model. CoRR [abs/1605.03170](#) (2016)
34. Insaftudinov, E., Andriluka, M., Pishchulin, L., Tang, S., Levinkov, E., Andres, B., Schiele, B.: Articulated multi-person tracking in the wild. CoRR [abs/1612.01465](#) (2016)
35. Kocabas, M., Karagoz, S., Akbas, E.: Multiposenet: Fast multi-person pose estimation using pose residual network. CoRR [abs/1807.04067](#) (2018)
36. Chen, L., Papandreou, G., Kokkinos, I., Murphy, K., Yuille, A.L.: Deeplab: Semantic image segmentation with deep convolutional nets, atrous convolution, and fully connected crfs. CoRR [abs/1606.00915](#) (2016)
37. Chen, L., Yang, Y., Wang, J., Xu, W., Yuille, A.L.: Attention to scale: Scale-aware semantic image segmentation. CoRR [abs/1511.03339](#) (2015)
38. Zhao, H., Shi, J., Qi, X., Wang, X., Jia, J.: Pyramid scene parsing network. CoRR [abs/1612.01105](#) (2016)
39. Lin, T., Dollár, P., Girshick, R.B., He, K., Hariharan, B., Belongie, S.J.: Feature pyramid networks for object detection. CoRR [abs/1612.03144](#) (2016)
40. Yang, W., Li, S., Ouyang, W., Li, H., Wang, X.: Learning feature pyramids for human pose estimation. CoRR [abs/1708.01101](#) (2017)
41. Chen, Y., Wang, Z., Peng, Y., Zhang, Z., Yu, G., Sun, J.: Cascaded pyramid network for multi-person pose estimation. CoRR [abs/1711.07319](#) (2017)

42. Badrinarayanan, V., Kendall, A., Cipolla, R.: Segnet: A deep convolutional encoder-decoder architecture for image segmentation. *IEEE Transactions on Pattern Analysis and Machine Intelligence* **39** (2017) 2481–2495
43. Ronneberger, O., Fischer, P., Brox, T.: U-net: Convolutional networks for biomedical image segmentation. *CoRR* [abs/1505.04597](#) (2015)
44. Noh, H., Hong, S., Han, B.: Learning deconvolution network for semantic segmentation. *CoRR* [abs/1505.04366](#) (2015)
45. Pohlen, T., Hermans, A., Mathias, M., Leibe, B.: Full-resolution residual networks for semantic segmentation in street scenes. *CoRR* [abs/1611.08323](#) (2016)
46. Zhou, Z., Siddiquee, M.M.R., Tajbakhsh, N., Liang, J.: Unet++: A nested u-net architecture for medical image segmentation. *CoRR* [abs/1807.10165](#) (2018)
47. Lin, G., Milan, A., Shen, C., Reid, I.D.: Refinenet: Multi-path refinement networks for high-resolution semantic segmentation. *CoRR* [abs/1611.06612](#) (2016)
48. Peng, C., Zhang, X., Yu, G., Luo, G., Sun, J.: Large kernel matters - improve semantic segmentation by global convolutional network. *CoRR* [abs/1703.02719](#) (2017)
49. Zhang, Z., Zhang, X., Peng, C., Cheng, D., Sun, J.: Exfuse: Enhancing feature fusion for semantic segmentation. *CoRR* [abs/1804.03821](#) (2018)
50. Chen, L., Zhu, Y., Papandreou, G., Schroff, F., Adam, H.: Encoder-decoder with atrous separable convolution for semantic image segmentation. *CoRR* [abs/1802.02611](#) (2018)
51. Xiao, T., Liu, Y., Zhou, B., Jiang, Y., Sun, J.: Unified perceptual parsing for scene understanding. *CoRR* [abs/1807.10221](#) (2018)
52. Fu, J., Liu, J., Wang, Y., Lu, H.: Stacked deconvolutional network for semantic segmentation. *CoRR* [abs/1708.04943](#) (2017)
53. Bulat, A., Tzimiropoulos, G.: Binarized convolutional landmark localizers for human pose estimation and face alignment with limited resources. *CoRR* [abs/1703.00862](#) (2017)
54. Chu, X., Yang, W., Ouyang, W., Ma, C., Yuille, A.L., Wang, X.: Multi-context attention for human pose estimation. *CoRR* [abs/1702.07432](#) (2017)
55. Ke, L., Chang, M., Qi, H., Lyu, S.: Multi-scale structure-aware network for human pose estimation. *CoRR* [abs/1803.09894](#) (2018)
56. Tang, W., Yu, P., Wu, Y. In: *Deeply Learned Compositional Models for Human Pose Estimation: 15th European Conference, Munich, Germany, September 8-14, 2018, Proceedings, Part III.* (2018) 197–214
57. Xiao, B., Wu, H., Wei, Y.: Simple baselines for human pose estimation and tracking. *CoRR* [abs/1804.06208](#) (2018)
58. Saxena, S., Verbeek, J.: Convolutional neural fabrics. *CoRR* [abs/1606.02492](#) (2016)
59. Zhou, Y., Hu, X., Zhang, B.: Interlinked convolutional neural networks for face parsing. *CoRR* [abs/1806.02479](#) (2018)
60. Fourure, D., Emonet, R., Fromont, E., Muselet, D., Tremau, A., Wolf, C.: Residual conv-deconv grid network for semantic segmentation. (2017)
61. Huang, G., Chen, D., Li, T., Wu, F., van der Maaten, L., Weinberger, K.Q.: Multi-scale dense convolutional networks for efficient prediction. *CoRR* [abs/1703.09844](#) (2017)
62. Wang, J., ke, S., Cheng, T., Jiang, B., Deng, C., Zhao, Y., Liu, D., Mu, Y., Tan, M., Wang, X., Liu, W., Xiao, B.: Deep high-resolution representation learning for visual recognition. (2019)

63. Sun, K., Zhao, Y., Jiang, B., Cheng, T., Xiao, B., Liu, D., Mu, Y., Wang, X., Liu, W., Wang, J.: High-resolution representations for labeling pixels and regions. CoRR [abs/1904.04514](#) (2019)
64. He, K., Zhang, X., Ren, S., Sun, J.: Deep residual learning for image recognition. CoRR [abs/1512.03385](#) (2015)
65. Simonyan, K., Zisserman, A.: Very deep convolutional networks for large-scale image recognition (2014)
66. Radosavovic, I., Kosaraju, R.P., Girshick, R., He, K., Dollr, P.: Designing network design spaces (2020)
67. Tan, M., Pang, R., Le, Q.V.: Efficientdet: Scalable and efficient object detection (2019)
68. Deng, J., Dong, W., Socher, R., Li, L.J., Li, K., Fei-Fei, L.: ImageNet: A Large-Scale Hierarchical Image Database. In: CVPR09. (2009)
69. Krizhevsky, A.: Learning multiple layers of features from tiny images. Technical report (2009)
70. Krizhevsky, A., Sutskever, I., Hinton, G.E.: Imagenet classification with deep convolutional neural networks. In: Proceedings of the 25th International Conference on Neural Information Processing Systems - Volume 1. NIPS12, Red Hook, NY, USA, Curran Associates Inc. (2012) 10971105
71. Ruder, S.: An overview of gradient descent optimization algorithms. CoRR [abs/1609.04747](#) (2016)
72. Glorot, X., Bengio, Y.: Understanding the difficulty of training deep feedforward neural networks. In Teh, Y.W., Titterton, M., eds.: Proceedings of the Thirteenth International Conference on Artificial Intelligence and Statistics. Volume 9 of Proceedings of Machine Learning Research., Chia Laguna Resort, Sardinia, Italy, PMLR (2010) 249–256
73. Ge, R., Kakade, S.M., Kidambi, R., Netrapalli, P.: The step decay schedule: A near optimal, geometrically decaying learning rate procedure. CoRR [abs/1904.12838](#) (2019)
74. Kingma, D.P., Ba, J.: Adam: A method for stochastic optimization. CoRR [abs/1412.6980](#) (2015)